International Journal of Scientific Research in Engineering and Management (IJSREM)
Volume: 05 Issue: 07 | July - 2021 ISSN: 2582-3930

SIMULATION OF 6KW VARIABLE DUTY CYCLE CONTROL BOOST PFC TOPOLOGY IN DISCONTINUOUS CURRENT MODE

Akkela Krishnaveni [1], Mahender Kodela [2].

[1] *M.Tech scholar, Department of EEE, Vaagdevi college of Engineering (Autonomous), Warangal.*
[2] *Assistant Professor, Department of EEE, Vaagdevi college of Engineering (Autonomous), Warangal.*

Abstract - *the conventional boost PFC converter was applied in continuous current mode due to current would operate continuously to obtain a high efficiency. A boost PFC converter in DCM control approach was investigated in this paper with a 6kW experiment. The operational principles of proposed DCM boost pfc converter was discussed first. And then relationships between inductor current and duty cycle as well as output voltage with duty cycle are evaluated. A modelling control scheme of boost pfc converter are derived through theoretical analysis and relationships of input current and input voltage. At the end, a 6kW prototype is investigated through combination of theoretical design and calculation, the prototype was able to achieve power factor correction which obtains a power factor of 0.99. In addition, the DCM control approach was demonstrated properly during the research.*

Key Words: ***Index Terms***—*Discontinuous current mode (DCM), power factor correction (PFC), variable-duty-cycle control.*

1. INTRODUCTION

Most applications requiring ac-dc power converters need the output dc voltage to be well regulated with good steady-state and transient performance. The circuit typically favored until recently (diode rectifier-capacitor filter) for the utility interface is cost effective, but it severely deteriorates the quality of the utility supply thereby affecting the performance of other loads connected to it besides causing other well known problems. In order to maintain the quality of the utility supply, several national and international agencies have started imposing standards and recommendations for electronic instrument connected to the utility. Since the mid-1980's power electronics engineers have been developing new approaches for better utility interface, to meet these standards. These new circuits have been collectively called Power factor correction (PFC) circuits.

With the increase of consumer electronics the power quality becomes poor. The reactive power drawn from the supply is increasing. This is because of the use of rectification of the AC input and the use of a bulk capacitor directly after the diode bridge rectifier. Reducing the input current harmonics to meet the agency standards implies improvement of power factor as well. For this reason the publications reported in this area have used "Power factor correction methods" and "Harmonic elimination/reduction methods" almost inter changeably. Several techniques for PFC and harmonic reduction have been reported and a few of them have gained greater acceptance over the others.

This chapter discusses the i) Nonlinear loads and their effect on the electricity distribution network, ii) Standard IEC and IEEE regulation for harmonics, iii) Power factor correction and its benefits, iv) application of PFC both for linear and non-linear loads, v) research background, vi) aim of the dissertation.

1.1 NONLINEAR LOADS AND THEIR EFFECT ON THE ELECTRICITY DISTRIBUTION NETWORK:

The instrument connected to an electricity distribution network usually needs some kind of power conditioning, typically rectification, which produces a non-sinusoidal line current due to the non-linear input characteristic. Line-frequency diode rectifiers convert AC input voltage into DC output voltage in an uncontrolled manner. Single-phase diode rectifiers are needed in relatively low power instrument that needs some kind of power conditioning, such as electronic instrument and household appliances. For higher power, three-phase diode rectifiers are used. In both single and three-phase rectifiers, a large filtering capacitor is connected across the rectifier output to obtain DC output voltage with low ripple. As a consequence, the line current is non sinusoidal. In most of these cases, the amplitude of odd harmonics of the line current is considerable with respect to the fundamental. While the effect of a single low power nonlinear load on the network can be considered negligible, the cumulative effect of several nonlinear loads is important. Line current harmonics have a number of undesirable effects on both the distribution network and consumers.

Distortion of the line voltage via the line impedance shown in Fig.1.1 where the typical worst case values: R-Line=0.5 ohm, and L-Line=1mH have been considered. The effect is stronger in weaker grids. For example, some electronic instrument is dependent on accurate determination of aspects of the voltage wave shape, such as amplitude, RMS and zero-crossings

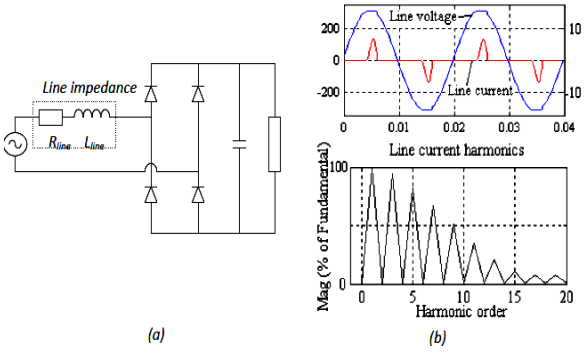

Fig. 1.1: Single-phase diode bridge rectifier: (a) Schematic; (b) Typical line voltage and line current waveforms (upper plot) and odd line current harmonics (lower plot). And the line current has THDi=1.5079 and power factor of 0.5475.

2. POWER FACTOR CORRECTION:

Reduction of line current harmonics is needed in order to comply with the standard. This is commonly referred to as the Power Factor Correction - PFC, which may be misleading. When an electric load has a PF lower than 1, the apparent power delivered to the load is greater than the real power that the load consumes. Only the real power is capable of doing work, but the apparent power determines the amount of current that flows into the load, for a given load voltage.

Power factor correction (PFC) is a technique of counteracting the undesirable effects of electric loads that create a power factor PF that is less than 1.

The power factor is defined as the ratio of the active power P to the apparent power S:

$$PF = P/S \tag{1.1}$$

For purely sinusoidal voltage and current, the classical definition is obtained:

$$pf = \cos\phi \tag{1.2}$$

Where osΦ is the displacement factor of the voltage and current. In classical sense, PFC means compensation of the "displacement factor".

The line current is non-sinusoidal when the load is nonlinear. For sinusoidal voltage and non sinusoidal current the PF can be expressed as.

$$PF = \frac{V_{rms} I_{1rms}}{V_{rms} I_{rms}} \cos\phi = \frac{I_{1rms}}{I_{rms}} \cos\phi = K_p \cos\phi \tag{1.3}$$

$$K_p = \frac{I_{1rms}}{I_{rms}}, K_p \in [0,1] \tag{1.4}$$

K_p describes the harmonic content of the current with respect to the fundamental. Hence, the power factor depends on both harmonic content and displacement factor. K_p is referred to as purity factor or distortion factor.

The total harmonic distortion factor THD_i is defined as

$$THD_i = \frac{\sqrt{\sum_{n=2}^{\infty} I_{n,rms}^2}}{I_{1rms}} \tag{1.5}$$

Hence the relation between Kp and THDi

$$K_p = \frac{1}{\sqrt{1+THD^2}} \tag{1.6}$$

Standard IEC 1000-3-2 sets limits on the harmonic content of the current but does not specifically regulate the purity factor Kp or the total harmonic distortion of the line current THD_i. The values of Kp and THD_i for which compliance with IEC 1000-3-2 is achieved depend on the power level. For low power level, even a relatively distorted line current may comply with the standard. In addition to this, it can be seen from (1.6) that the distortion factor Kp of a waveform with a moderate THD_i is close to unity (e.g. Kp=0.989 for THDi=15%). Considering (1.3) as well, the following statements can be made:

1. Power factor PF is not significantly degraded by harmonics, unless their amplitude is quite large (low K_p, very large THD_i).

2. Low harmonic content does not guarantee high power factor (K_p close to unity, but low cosΦ).

2.1 PASSIVE PFC CONVERTR:

Passive PFC methods use only passive elements in addition to the diode bridge rectifier, to improve the shape of the line current. As mentioned in the previous chapter, the diode bridge rectifier, shown again in Fig.2.1 (a), has non-sinusoidal line current. This is because most loads require a supply voltage with low ripple, which is obtained by using a correspondingly large capacitance the output capacitor Cf. Consequently, the conduction intervals of the rectifier diodes are short and the line current consists of narrow pulses with an important harmonic content.

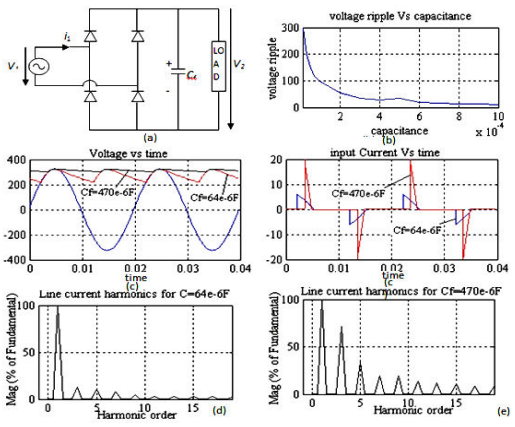

Fig. 2.1 Diode bridge rectifier: (a) Schematic; (b) Voltage ripple as a function of the output filter capacitance; (c) Line voltage and output voltage (upper plot), and input current (lower plot),with V1=230Vrms 50Hz and constant power load P = 200W . With Cf = 470µF, the line current has Kp = 0.4349, cosΦ = 0.9695 and PF =0.4216, and the output voltage ripple is V2 =25V. With Cf = 64µF, the line current has Kp = 0.6842, cosΦ = 0.8805 and PF =0.6024, and the output voltage ripple is V2 =105V; (d) and (e) Line current harmonics with Cf=64µF and Cf =470µF respectively.

The simplest way to improve the shape of the line current, by adding additional components, is to use a lower capacitance of the output capacitor Cf. When this is done, the ripple of the output voltage increases and the conduction intervals of the rectifier diodes widen. The shape of the input current depends on the type of load that the rectifier is supplying. The shape of the input current is improved to a certain extent with the lower capacitance, at the expense of increased output voltage ripple, which can be seen from the results listed in the caption of Fig. 2.1. The concept is highlighted by the simulated waveforms shown in Fig. 2.1c), for two values of the output capacitor and assuming constant power load.

2.2 ACTIVE PFC CONVERTR:

An active PFC in a power electronic system controls the amount of power drawn by a load in order to obtain a power factor as close as possible to unity. In most applications, the active PFC controls the input current of the load so that the current waveform is proportional to the mains voltage waveform (a sine wave). Active switches are used in conjunction with reactive elements in order to increase the effectiveness of the line current shaping and to obtain controllable output voltage. The switching frequency further differentiates the active PFC solutions into two classes.

1. Low frequency active PFC: Switching takes place at low-order harmonics of the line-frequency and it is synchronized with the line voltage.

2. High frequency active PFC: The switching frequency is much higher than the line frequency.

3. MODELLING AND CONTROL SCHEME

The proposed boost PFC control strategy contains two control loops while its operating under discontinuous current mode, which are voltage loop and current loop. By applying small signal modelling approach to establish mathematical functions between input current with duty cycle, output voltage with duty cycle.

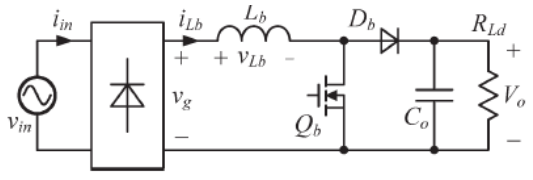

Fig. 3.1 boost PFC converter

Fig. 3.1 shows the main circuit of a boost PFC converter. For simplicity, the following assumptions are made: 1) All the devices and components are ideal; 2) the ripple of the output voltage is too small to be neglected; and 3) the switching frequency is much higher than the line frequency.

Supposing that the input voltage is purely sine waveform and it has no distortion, the input voltage is defined as

$$v_{in}(t) = V_m \sin \omega t \quad \ldots\ldots\ldots\ldots \quad (3.1)$$

Where V_m is the amplitude of the input voltage and ω is the angular frequency of the input voltage.

Then, the rectified voltage is

$$v_g = V_m |\sin \omega t| \quad \ldots\ldots\ldots\ldots \quad (3.2)$$

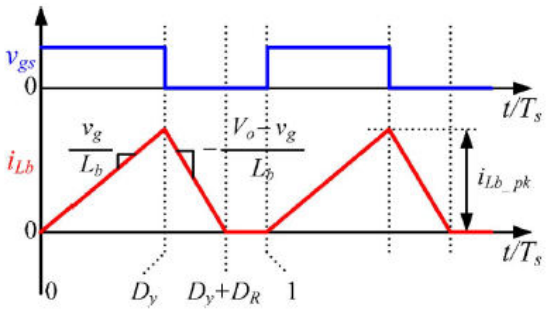

Fig. 3.2 shows the inductor current waveform in a switching cycle when the converter operates in DCM. In a switching cycle, the inductor peak current i_{Lb}_pk is

$$i_{Lb\_pk}(t) = \frac{v_g}{L_b} D_y T_s = \frac{V_m |\sin \omega t|}{L_b} D_y T_s \quad \ldots.(3.3)$$

Where D_y is the duty cycle and T_s is the switching cycle.

In each switching cycle, the inductor has a volt-second balance, i.e.,

$$v_g D_y T_s = (V_o - v_g) D_R T_S \quad \ldots\ldots\ldots\ldots \quad (3.4)$$

Where V_o is the output voltage and D_R is the duty cycle corresponding to the reset time of the inductor current.

Equation (4) can be rewritten as

$$D_R = \frac{v_g}{V_o - v_g} D_y = \frac{V_m |\sin \omega t|}{V_o - V_m |\sin \omega t|} D_y \ldots(3.5)$$

From (3) and (5), the average inductor current in a switching cycle can be derived as

$$i_{Lb\_av}(t)=\frac{1}{2}i_{Lb\_pk}(t)(D_y+D_R)=\frac{V_m D_y^2}{2L_b f_s}\frac{|\sin\omega t|}{1-\frac{V_m}{V_o}|\sin\omega t|}D_y \quad \ldots (3.6)$$

Where $f_s = 1/T_s$ is the switching frequency.

Thus, the input current is

$$i_{in}(t)=\frac{V_m D_y^2}{2L_b f_s}\frac{\sin\omega t}{1-\frac{V_m}{V_o}|\sin\omega t|} \quad \ldots\ldots \quad (3.7)$$

When D_y is constant, according to (3) and (6),

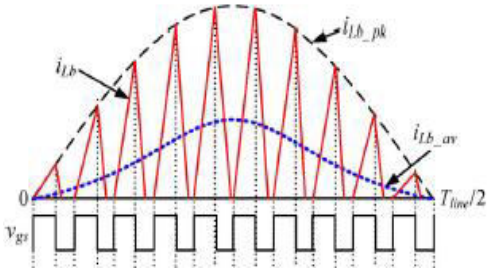

Fig. 3.3. Inductor current waveform in a half line cycle.

Fig..3 shows the instantaneous waveform, the peak value envelope, and the average value of the inductor current. It can be seen that the shape of the peak inductor current is sinusoidal; however, the shape of the average inductor current is not sinusoidal, and there is distortion in it.

For analysis simplicity, the average inductor current is normailed with the base of

$(V_m D_y^2/2L_b f_s)(1/(1-V_m/V_o))$, so (7) is rewritten as

$$i_{in}^*=\left(1-\frac{V_m}{V_o}\right)\frac{\sin\omega t}{1-\frac{V_m}{V_o}|\sin\omega t|} \quad \ldots\ldots\ldots\ldots (3.8)$$

According to (8), the normalized average inductor current is shown in Fig. 4, from which it can be seen that the shape of the average inductor current is only dependent on V_m/V_o, and the smaller the V_m/V_o is, the closer to sinusoidal the current shape is. This can be explained as follows. As the duty cycle is constant in a line cycle, the peak value of the inductor current is in the sinusoidal shape, and the average value of the inductor current in the rising period is sinusoidal. However, the falling time of the inductor current is dependent on the value of $(V_o - v_g)$, and it varies with v_g, so the average value of the inductor current in the falling period is not sinusoidal. Thus, the average value of the inductor current in a switching cycle is not sinusoidal. The smaller the V_m/V_o is, the shorter the falling time of the inductor current is and, thus, the closer to sinusoidal shape the average inductor current in a switching cycle is.

From (1) and (7), the average input power is derived as

$$P_{in}=\frac{1}{T_{line}/2}\int_0^{\frac{T_{line}}{2}} v_{in}(t)i_{in}(t)dt$$
$$=\frac{V_m^2 D_y^2}{2L_b f_s}\frac{1}{\pi}\int_0^{\pi}\frac{\sin^2\omega t}{1-\frac{V_m}{V_o}|\sin\omega t|}d\omega t \quad \ldots \quad (3.9)$$

Where T_{line} is the line cycle [17].

Assuming that the efficiency of the converter is 100%, i.e., $P_{in} = P_o$, the duty cycle is

$$D_y=\frac{1}{V_m}\sqrt{\frac{2L_b f_s \pi P_o}{\int_0^{\pi}\frac{\sin^2\omega t}{1-\frac{V_m}{V_o}|\sin\omega t|}d\omega t}} \quad \ldots\ldots (3.10)$$

From (7) and (9), the input PF can be derived as [16]

$$PF=\frac{P_{in}}{\frac{1}{\sqrt{2}}V_m I_{in\_rms}}$$

$$=\frac{P_{in}}{\frac{1}{\sqrt{2}}V_m\sqrt{\frac{1}{\pi}\int_0^{\pi}(i_{in}(t))^2 d\omega t}}$$

$$=\frac{\sqrt{\frac{2}{\pi}}\int_0^{\pi}\frac{\sin^2\omega t}{1-\frac{V_m}{V_0}|\sin\omega t|}d\omega t}{\sqrt{\int_0^{\pi}\left(\frac{\sin\omega t}{1-\frac{V_m}{V_0}|\sin\omega t|}\right)^2 d\omega t}} \quad \ldots\ldots\ldots\ldots (3.11)$$

Where I_{in}_rms is the rms value of the input current.

According to (11), the input PF is plotted as shown in Fig. 5. It can be seen that the larger the V_m/V_o is, the lower the PF is. If V_m/V_o is greater than 0.9, the PF is less than 0.9. When the output voltage is 400 V, the PF is only 0.865 at an input voltage of 264 VAC, which is not satisfied with the regulation standard such as EN61000-3-2

3.3 DCM BOOST PFC CONVERTER WITH VARIABLE-DUTY-CYCLE CONTROL

3.3.1 Variable Duty Cycle for PF = 1

By observing (7), in order to achieve a unity PF, the duty cycle should be variable as

$$D_y = D_0\sqrt{1-\frac{V_m}{V_0}|\sin\omega t|} \quad \text{.....(3.12)}$$

where D_0 is a coefficient, which will be explained later.

Substitution of (12) into (7) leads to

$$i_{in}(t) = \frac{V_m D_0^2 \sin\omega t}{2L_b f_s} \quad \text{.....} \qquad (3.13)$$

From (13), it can be seen that if the duty cycle varies as (12), the shape of the input current is sinusoidal and the PF is unity.

From (1) and (13), the average input power is derived as

$$P_{in} = \frac{1}{2}V_m\frac{V_m D_0^2}{2L_b f_s} = \frac{V_m^2 D_0^2}{4L_b f_s} = P_0 \text{.....} \qquad (3.14)$$

From (14), D_0 can be obtained as

$$D_0 = 2\sqrt{P_o L_b f_s}\Big/V_m \quad \text{.....} \qquad (3.15)$$

Substitution of (15) into (12) leads to

$$D_y = \frac{2\sqrt{P_o L_b f_s}}{V_m}\sqrt{1-\frac{V_m}{V_o}|\sin\omega t|}$$

$$= \frac{2\sqrt{P_o L_b f_s}}{V_m}\sqrt{1-\frac{V_m}{V_o}} \quad \text{.....} \qquad (3.16)$$

Equation (16) implies that if the duty cycle is a function of the rectified input voltage v_g , the input PF of the DCM boost PFC converter is unity.

3.3.2 Fitting Duty Cycle

The duty cycle expressed in (16) is complicated to implement because a multiplier, a divider, and a square-root extractor are needed; it is necessary to seek a function that fits (16), which can be more easily implemented.

Defining $a = V_m/V_o$, $y = |\sin\omega t|$, (12) can be rewritten as

$$D_y = D_o\sqrt{1-ay} \quad \text{.....} \qquad (3.17)$$

Based on Taylor's serie

$$f(x) = f(x_o) + f'(x_o)(x-x_o) + \frac{1}{2!}f''(x_o)(x-x_o)^2 + \text{.....} + \frac{1}{n!}f^n(x_o)(x-x_o)^n + \text{...}$$

(3.18)

Equation (17) can be expressed as

$$D_y = D_o\left[\sqrt{1-ay_o} - \frac{a}{2}(1-ay_o)^{-\frac{1}{2}}(y-y_o) - \frac{1}{2!}\frac{a^2}{4}(1-ay_o)^{-\frac{3}{2}}(y-y_o) + \text{.....}\right]\cdots$$

(3.19)

Reserving only the first derivative item, (19) is approximated as

$$D_{y\_fit} = D_o\left[\sqrt{1-ay_o} - \frac{a}{2}(1-ay_o)^{-\frac{1}{2}}(y-y_o)\right]$$

$$= D_1\left(1-\frac{a}{2-ay_o}y\right) \quad \text{.....} \qquad (3.20)$$

Where $D_1 = \left(D_o(2-ay_o)\right)\Big/\left(2\sqrt{1-ay_o}\right)$

Substitution of (20) into (7) and (9), respectively, leads to

$$i_{in} = \frac{V_m D_1^2}{2L_b f_s}\frac{\sin\omega t}{1-a|\sin\omega t|}\left(1-\frac{a}{2-ay_o}|\sin\omega t|\right)^2 \quad \text{.....}$$

…. (3.21)

$$P_{in} = P_o$$

$$= \frac{V_m^2 D_1^2}{2L_b f_s}\int_0^{\pi}\frac{\sin^2\omega t\left(1-\frac{a}{2-ay_o}|\sin\omega t|\right)^2}{1-a|\sin\omega t|}d\omega t \quad \text{.....}$$

..... (3.22)

From (21) and (22), the input PF is calculated as

$$PF = \frac{P_{in}}{V_{in\_rms}I_{in\_rms}}$$

$$= \frac{P_{in}}{\frac{1}{\sqrt{2}} V_m \sqrt{\frac{1}{T_{line}/2} \int_0^{T_{line}/2} i_{in}^2(t)dt}}$$

$$= \frac{\sqrt{\frac{2}{\pi}} \int_0^{\pi} \frac{\sin^2 \omega t \left(1 - \frac{a}{2 - ay_o} |\sin \omega t|\right)^2}{1 - a|\sin \omega t|} d\omega t}{\sqrt{\int_0^{\pi} \frac{\sin^2 \omega t \left(1 - \frac{a}{2 - ay_o} |\sin \omega t|\right)^2}{(1 - a|\sin \omega t|)^2} d\omega t}} \quad \cdots (3.23)$$

The input PF is shown in Fig. 6 according to (23). It can be seen that when a is small, the input PF is almost constant and is very close to unity as y_0 varies from 0 to 1. When a increases, the influence of y_0 on the input PF increases. Thus, the value of y_0, which enables the maximum input PF at the highest input voltage, is chosen to ensure the input PF to be close to 1 over the whole input-voltage range. For the input-voltage range of 90-264 √AC, the output voltage is set to 400 V. Substituting a=2642/400 into (23) and then differentiating (23) with y_0 and setting it to zero, $y_0 = 0.866$ is obtained.

Substituting $y_0 = 0.866$ into (20), the duty cycle is ex pressed as

$$D_{y\_fit} = D_1 \left(1 - \frac{a}{2 - ay_0} y\right)$$

$$= D_1 \left(1 - \frac{V_m |\sin \omega t|}{2V_o - 0.866V_m}\right)$$

$$= D_1 \left(\frac{2V_o - 0.866V_m - V_m |\sin \omega t|}{2V_o - 0.866V_m}\right) \quad \ldots\ldots\ldots\ldots (3.24).$$

4. DCM BOOST PFC CONVERTER WITH VARIABLE-DUTY-CYCLE

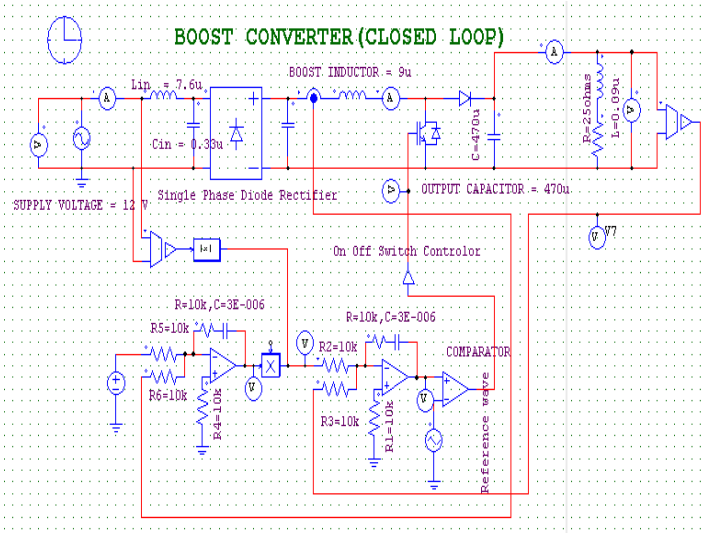

Fig.3.7 DCM Boost PFC converter with Variable-duty-cycle control-R-L Load

4.1 Simulation waveforms

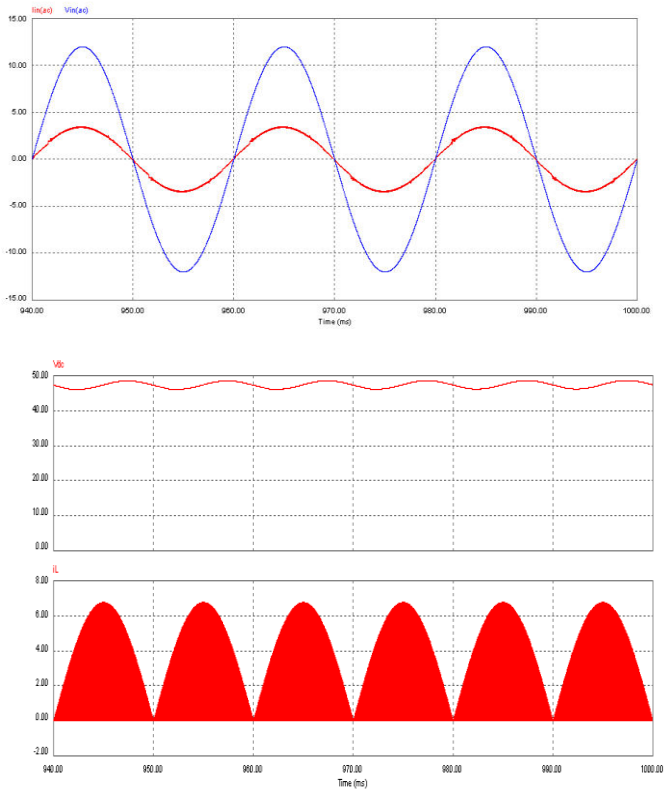

Fig.6.8 (a) input voltage and current (b) output voltage (c) Boost inductor current waveforms with Variable-duty-cycle control boost converter-R-L Load

4.2.2.3 Comments:

Fig3.8 (a) Shows input voltage and current waveform form this we can observe that the input power factor is 0.9984 only Fig.3.8 (b) Shows output voltage waveforms with Variable-duty-cycle

control in this the voltage ripple is 2% Fig.6.8 (c) Shows Boost inductor current waveforms here the switching frequency is 100khz and the inductor Current is zero for each switching interval.

5.CONCLUSION

In DICM, the input inductor is no longer a state variable since its state in a given switching cycle is independent on the value in the previous switching cycle. The peak of the inductor current is sampling the line voltage automatically. This property of DICM input circuit can be called “self power factor correction” because no control loop is required from its input side.

We can conclude that the basic boost converter and buck-boost converter have excellent self PFC capability naturally. Among them, boost converter is especially suitable for DICM PFC usage and buck-boost is not widely used because of the drawbacks such as: the input voltage and the output voltage don’t have a common ground due to the reversed output voltage polarity, etc. Hence, this converter is the most preferable by the designers for the power factor correction purpose. Other converters may be used only if their input V-I characteristics have been modified (linear zed), or when they operate in a continuous inductor conduction mode.

In addition, if the discontinuous inductor current mode is applied, the input current is normally a train of triangle pulse with nearly constant duty ratio. In this case, an input filter is necessary for smoothing the pulsating input current into a continuous one.

To conclude, a 500 W, 40 kHz variable duty cycle DCM boost PFC converter has been analyzed, simulated and results are validated with experimental results. The proposed converter gives around 0.9977 (almost unity) power factor with an efficiency of around 98%.

6.FUTURE WORK

For further improvement, we can introduce predictive control strategy in which the active filtering approach can be utilized so as to further reduce the current ripples and switching losses. The switches can be made to be work under soft-switching condition.

7.REFERENCES

[1] Lu B, Brown R, Soldano M. Bridgeless PFC implementation using one cycle control technique. Twentieth Annual IEEE APEC 2005.

[2] IEC61000-3-2: 1995, Electromagnetic compatibility Part3: limits-set.2: limits for harmonic current emission (equipment input current≤16A per phase).

[3] IEC61000-3-12: 2005, Electromagnetic compatibility (EMC) Part3-2: limits-limits for harmonic currents produced by equipment connected to public low-voltage systems with input current > 16 A and ∟75 A per phase.

[4] S.Buso, P.Mattaveli. Simple Digital Control Improving Dynamic Performance of Power Factor Preregulator[J]. IEEE Transactions on Power Electronics, 1997, 13(2): 814-823.

[5] Zaohong Yang, Paresh C.sen. A Novel Technique to Achieve Unity Power Factor and Fast Transient Response in AC-to-DC Converter [J]. IEEE Transacdonsons on Power Electronics,2001, 16(6):137-143.

[6] Koen De Gusseme. Control Active Power Factor Correction Converters[J]. RUG-FTW, 2nd PhD Symposium, 2001, 18(24): 1-2.

[7] A. F de Souza, and 1. Barbi, "High power factor rectifier with reduced conduction and commutation losses, " in Proc. IEEE Telecommunication Energy Conference, Jun. 1999.

[8] Jinjun Liu, F.C, Weiyun Chen, FC, Jindong Zhang, F.e., Dehong Xu and FC. Lee, "Evaluation of power losses in different CCM mode singlephase boost PFC converters via a simulation tool, " in Procs. IEEE lAC, Vol.4, pp.2455-2459 , Oct 2001.

[9] M. Shoyama, L. Ge, and T. Ninomiya, "Balanced switching converter to reduce common mode conducted noise, " in IEEE Trans. on Industrial Electronics, Vol. 50, no. 6, pp. 1095-1099, Dec. 2003

[10] M. Hongfei, X. Dianguo, and M. Lijie, “Suppression techniques of common mode voltage generated by voltage source PWM inverter,” in Proc. 4th Int. Power Electron. Motor Contr. Conf., 2004, vol. 3, pp. 1533–1538.

[11] N.K. Poon, J.C.P. Liu, C.K. Tse, and M.H Pong, “Techniques for Input Ripple Current Cancellation: Classification and Implementation,” IEEE Trans. Power Electron., vol. 15, no. 6, pp. 1144-1 152, Nov 2000.

[12] J. J. Casanova, Z. N. Low, and J. Lin, “A loosely coupled planar wireless power system for multiple receivers,” IEEE Trans. Ind. Electron., vol. 56, no. 8, pp. 3060–3068, Aug. 2009.

[13] B. Singh, B. N. Singh, A. Chandra, K. Al-Haddad, A. Pandey, and D. P. Kothari, “A review of single-phase improved power quality AC-DC converters,” IEEE Trans. Ind. Electron., vol. 50, no. 5, pp. 962–981,Oct. 2003.

[14] K. V. Iyer, R. Baranwal, and N. Mohan, “A High-Frequency AC-Link Single-Stage Asymmetrical Multilevel Converter for Grid Integration of Renewable Energy Systems,” IEEE Trans. Power Electron., vol. 32, no. 7, pp. 5087–5108, 2017

[15] B. Zhao, Q. Yu, and W. Sun, “Extended-Phase-Shift Control of Isolated Bidirectional DC–DC Converter for Power Distribution in Microgrid,” IEEE Trans. Power Electron., vol. 27, no. 11, pp. 4667–4680, 2012

[16] Crebier, J.e., Brunello, M. and Ferrieux, J.P., "A new method for EMI study in PFC rectifiers", Proc. iEEE Power Electronics Spc. Coni, PESC-20J J, pp. 855-860.